CrossMark

RESEARCH PAPER

Fabrication of pneumatic valves with spherical dome-shape fluid chambers

Chang Kyu Oh[1] · **Sang Wook Lee**[2] · **Ok Chan Jeong**[1,3]

Abstract This paper describes a simple fabrication method for pneumatic valves with spherical dome-shape fluidic chambers and channels. The proposed method is based on replicating a deformed polydimethylsiloxane (PDMS) diaphragm using a variable PDMS mold during the liquid PDMS curing process. A PDMS mold structure with a sealed cavity is prepared through a typical replica molding process and structural bonding with a glass substrate. The PDMS diaphragm inflates due to thermal expansion of air in the sealed cavity when it is placed on a hotplate during the thermal curing process, and this shape is transferred to liquid PDMS poured on the active PDMS structure. The proposed pneumatic valve can then be fabricated by bonding the valve chamber to the diaphragm. The effectiveness of the proposed valve was verified through optical observations of the valve pattern and measurements of the temporal response of the flow rate using pressurized liquid flow rectified by the fabricated valve. A finite element method was used to provide a structural analysis of the valve diaphragm to examine the characteristics of the rectified flow rate of the working fluid due to structural deformation of the valve diaphragm. The proposed fabricated valve effectively overcame the drawbacks of microfluid channels with rectangular cross sections and was also suitable for other micro-devices with spherical dome-shape cross sections.

Keywords Polydimethylsiloxane · Pneumatic valve · Spherical dome-shape fluidic chamber

✉ Ok Chan Jeong
memsoku@inje.ac.kr

1 Graduate School of Mechanical Engineering, Inje University, Gimhae, Republic of Korea

2 Department of Chemistry, The University of Tokyo, Tokyo, Japan

3 Department of Biomedical Engineering, Inje University, Gimhae, Republic of Korea

1 Introduction

Mechanical micro-valves are essential components for controlling fluid flow on a micro-fluidic platform. Various actuation methods for micro-valves fabricated using typical silicon-based micro-machining technology and polymer-based soft lithography have been reported, including magnetic (Yanagisawa et al. 1993; Bae et al. 2002; Oh et al. 2005), electrostatic (Sato and Shikida 1994; Goll et al. 1997; Yang et al. 2004), piezoelectric (Li et al. 2004; Yang et al. 2004; Goettsche et al. 2005), thermal (Ho et al. 1998; Rich and Wise 2003; Takao et al. 2005), and pneumatic (Sundararajan et al. 2005; Hosokawa and Maeda 2000; Grover et al. 2003).

There is great interest in fabricating pneumatically driven micro-valves by taking advantage of micro-fluidics and soft lithography processes (Whitesides 2006; McDonald and Whitesides 2002). This was first proposed by Quake's group (Unger et al. 2000; Thorsen et al. 2002; Studer et al. 2004). Polymeric micro-valves are easy to fabricate and integrate with other essential components. Compared with other methods or fabricating mechanical valves using external electrical or magnetic power sources, there is no unwanted thermal elevation due to operational methods, and mechanical damage can be prevented due to the soft and deformable contact of the polydimethylsiloxane (PDMS) membrane. Thus, various applications using pneumatic micro-valves have been

reported (Liu et al. 2002; Wang et al. 2004; Fu et al. 2002; Studer et al. 2004).

Pneumatic valves can be divided into two groups: those that are normally open (Unger et al. 2000) and those that are normally closed (Hosokawa and Maeda 2000). Normally open pneumatic valves are widely used because they are easy to fabricate, integrate, and operate. A typical normally open valve consists of a valve chamber, deformable membrane, and fluid channel. A thin membrane is inflated and seals the liquid chamber or channel using the pressure change in the valve chamber. However, typical normally open valves cannot fully close off the fluid flow because the liquid chamber or channel has a rectangular cross section. Thus, a simple and reliable method is required to fabricate curved micro-fluidic structures.

There have been some reports describing molds for fabricating micro-devices with rounded cross sections; possible techniques include making use of the multilayer soft lithography (MSL) using the thermal reflow process with photoresists (Unger et al. 2000; Thorsen et al. 2002; Studer et al. 2004; Dy et al. 2014), a photocurable oligomer (Park et al. 2010), the mechanical loading of a spherical object (Cherng and Su 2014), or an epoxy resin stamp (Huang et al. 2012). Among these techniques, MSL can provide a convenient and low-cost method for fabricating a replica mold with a curved profile. The effects of the positive photoresist thermal reflow process on the mold dimensions before and after the reflow process have been characterized comprehensively, as the curved cross section of the fluidic structure is important for valve performance (Fordyce et al. 2012). However, complex process designs and protocols of the positive photoresist thermal reflow process, such as the coating speed, baking time, and temperature, are also essential for the fabrication of replica molds with parabolic profiles. Moreover, the height of the curved profile of the mold structure is limited by the controllable maximum thickness of AX 50XT photoresist (~84 μm). Therefore, it is difficult to provide general solutions for other positive photoresists to fabricate curved mold structures because the reported method was based on the thermal reflow process of a specific photoresist. Another issue is that the curved shape of the micro-fluid channel at the valve location must closely match the physical shape of the deformed diaphragm, which has proved problematic, even when a fluid channel with a curved cross section is successfully fabricated using the proper curved mold structure. When the shapes do not match exactly, leakage of the fluid flow occurs since the valve diaphragm cannot close off perfectly. New approaches to fabricating highly sophisticated micro-valves are necessary to overcome this problem.

In this paper, a simple fabrication method for a curved PDMS structure is proposed. A pneumatically driven micro-valve with a spherical dome-shape fluidic chamber

was fabricated using the proposed method. The flow rate of the pressurized working fluid rectified by the proposed valve was measured under various operational pressures for the pneumatic valve, and the effectiveness of the proposed valve was analyzed through comparison of experimental results for a typical valve with a fluid chamber having a rectangular cross section.

2 Pneumatic valve with a spherical dome-shape liquid chamber

2.1 Valve structure

Figure 1 shows a schematic view of the pneumatic valve with a spherical dome-shape liquid chamber. It consists of three PDMS layers: the pneumatic actuator, the valve diaphragm, and the fluid channel/chamber layer. When external compressed air is supplied to the valve chamber, the
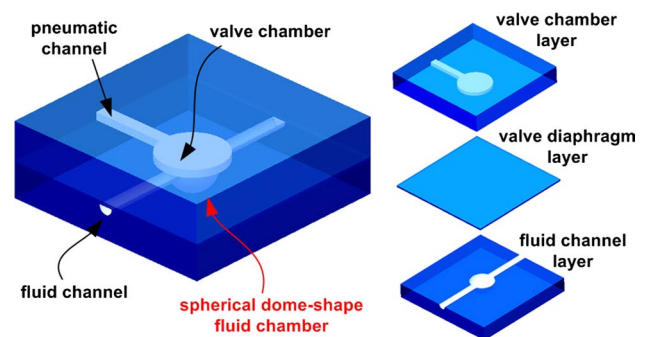

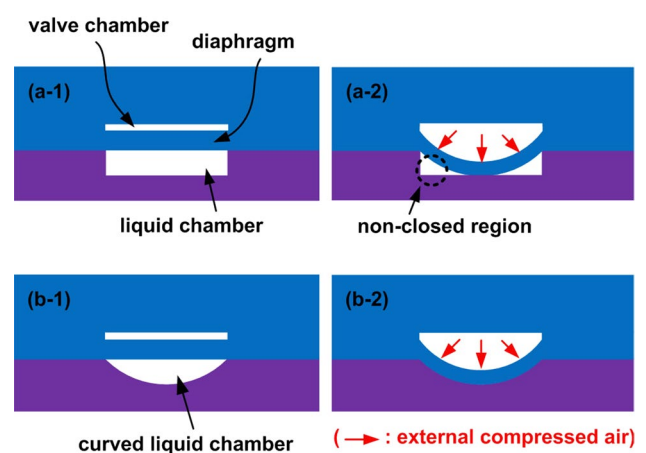**Fig. 1** Schematic view of the pneumatic valve with a spherical dome-shape liquid chamber

Fig. 2 **a** Structure and **b** deformed valve diaphragm of the (*1*) typical and (*2*) proposed pneumatic valves

flexible PDMS diaphragm inflates and impedes the liquid flow. The diameter of the valve chamber and liquid chamber are 900 and 650 μm, respectively. The width of the channel is 250 μm.

As shown in Fig. 2a, a normally open valve with a fluid chamber having a rectangular cross section does not fully close off the liquid flow; some regions around the corners of the rectangular chamber do not completely close. However, the deformed diaphragm of the proposed valve can close off the liquid flow effectively because it has a curved liquid chamber, as shown Fig. 2b. A nearly perfect liquid valve could be achieved if the physical shape of the round liquid chamber coincides with the fully inflated deformation of the valve diaphragm. However, considering the large deformation of the valve diaphragm of a pneumatic valve, it is difficult to fabricate such curved PDMS structures using a typical replica mold method with a photoresist. Therefore, a new approach to fabricating micro-fluidic structures with curved profiles is required.

2.2 Fabrication method

Figure 3 shows the fabrication process for the proposed micro-valve with a spherical dome-shape fluid chamber. First, 10 mL of the liquid 10:1 PDMS mixture (Sylgard 184, Dow Corning Inc.) for fabricating PDMS mold (layer 1) is poured onto a prepared SU-8 mold 55 μm thick for the fluid chamber, spun at 1500 rpm for 10 s, and then

cured for 30 min at 75 °C (a). In this work, all thermal heating processes were performed using a hotplate. The cured PDMS layer is cut with a knife manually (b), peeled off from the SU-8 mold, and then bonded with the slide glass substrate using the atmosphere plasma bonding method (c). The PDMS block, 2 mm thick, is also bonded again (d). Then, 2 mL of liquid PDMS for fabricating curved chamber (layer 2) is poured onto the prepared bonded structure (e). This is followed by curing the liquid PDMS using a typical hot plate (f). During the thermal curing process of liquid PDMS, the flexible PDMS diaphragm inflates due to thermal expansion of trapped air in the sealed cavity. The deformed shape of the PDMS diaphragm is transferred to the liquid PDMS layer. That is, this deformed diaphragm can act like a replicable mold. After curing for 30 min, the glass substrate is allowed to cool to room temperature. Then, the cured structure is cut with a knife (g). However, once the curing process has finished, there are no noticeable structures and/or interfacial layers, such as a single cured PDMS layer, on the cover glass substrate. Therefore, the printed layout of the fluid chamber structure is used as the reference cutting guideline. The slide glass substrate with the cured PDMS structure is placed onto it, aligned, and then the liquid chamber part is cut by taking advantage of the transparency of the structure. Rubbing the cutting surface gently with flat tip tweezers allows two cured PDMS layers to be recognized because they are separated locally. The newly cured PDMS layer with a curved liquid
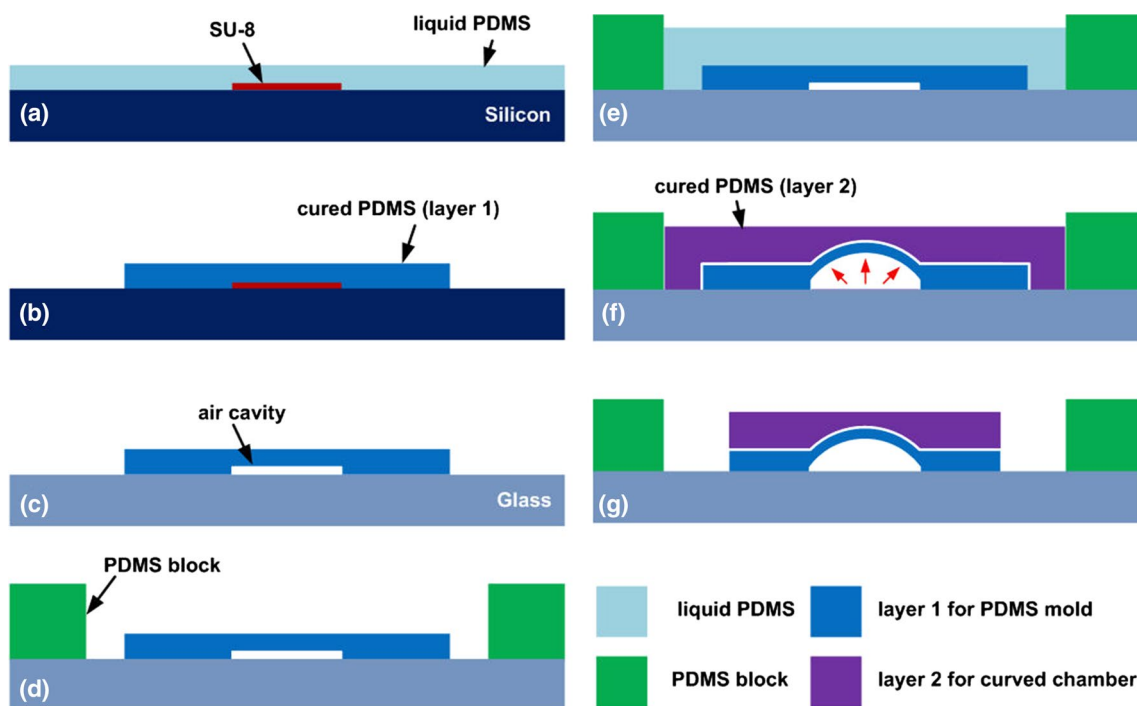

Fig. 3 Fabrication process for the proposed micro-valve with a spherical dome-shape fluid chamber
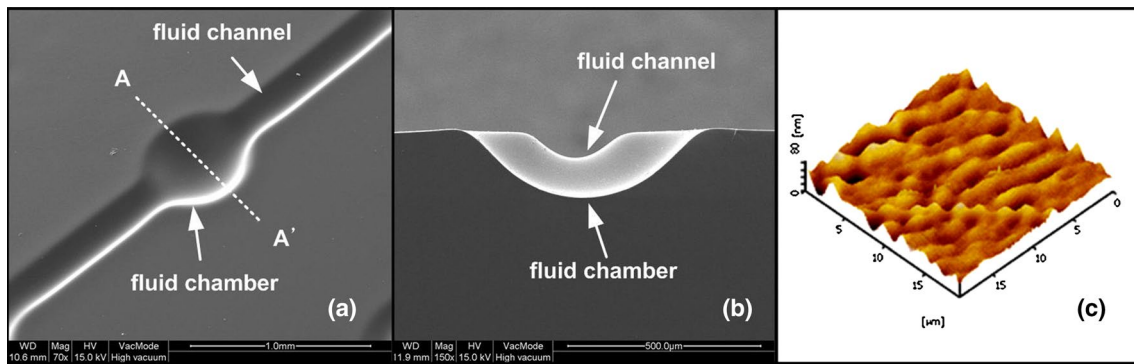
Fig. 4 SEM images of the replicated PDMS structure with **a** a spherical dome-shape fluid chamber connecting the fluid channel, **b** its cross section, and **c** AFM image of the replicated PDMS surface

chamber (layer 2) is then peeled off from the PDMS mold (layer 1) with flat tip tweezers. After the fabrication process of the fluid chamber, the micro-valve is assembled by the sequential bonding processes of the prepared valve chamber layer to the valve diaphragm layer and the fluid chamber layer, as shown in Fig. 1. First, the valve chamber layer is bonded with the valve diaphragm layer. The bonded structure and the fluid chamber layer are aligned using the printed layout of the valve structure under the microscope and then bonded again. For comparison, a valve structure with a rectangular liquid chamber was also fabricated using the same SU-8 mold and then tested.

2.3 Surface profile

Figure 4 illustrates the surface profiles of the fabricated spherical dome-shape fluid chamber measured with a surface profiler (Dektak 150M, VEECO Instrument). To understand the temperature-dependent deformed shape of the curved PDMS structure, the curved fluid chambers were fabricated under various curing temperatures and observed. The thickness of the active mold diaphragm was 51 μm, and the curing time was 30 min. The depth of the fluid chamber increased with increasing curing temperature. In our experience, liquid PDMS is not fully cured at 30 min when the curing temperature is 50 °C. However, when the curing temperature is 75–150 °C, excessive curing time (longer than 30 min) has very minor effects on the surface profile. Therefore, to ensure reliability of the fabrication process and ease of manual handling, we set the temperature and duration of the curing process for liquid PDMS at 150 °C and 30 min, respectively, as shown in Fig. 3.

Figure 5a, b shows SEM (Field Emission Gun Scanning Electron Microscope System, Quanta 200 FEG, FEI Company) images of the replicated PDMS structure with a spherical dome-shape fluid chamber connecting the fluid channel (a), as illustrated in Fig. 3h and its cross section

(b). The dimensions of the PDMS structure were measured using a digital microscope (Hi-Rox, KH-7700). When the thickness of the PDMS diaphragm of the active mold in Fig. 3b was 43 μm, the heights of the replicated PDMS structure for the spherical dome-shape fluid chamber and liquid channel were 150 and 40 μm, respectively. Compared with the height of the fluid chamber as shown in Figs. 4 and 5, the SEM image had the large deformation relatively. This phenomenon was mainly caused by the thickness of the PDMS mold diaphragm since the maximum deflection of the circular diaphragm is proportional to the cube root of the pressure in the sealed cavity and inversely proportional to the cube root of the thickness of the PDMS mold diaphragm (Jeong et al. 2004).

However, SEM observation revealed a wrinkling pattern on the PDMS surface. This was likely mainly caused by the compressive stress acting on the cured PDMS during shrinkage of the liquid PDMS during the thermal curing
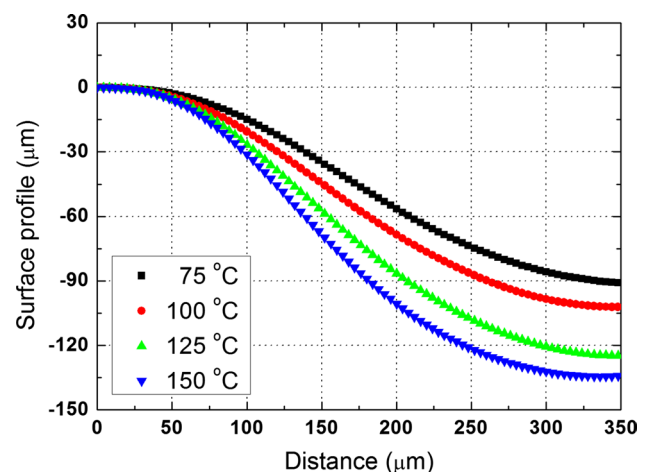

Fig. 5 Surface profiles of the fabricated spherical dome-shape fluid chamber under various curing temperatures

Table 1 Summary of surface roughness of PDMS surfaces

PDMS	R_a (nm)	P_v (nm)
Native	0.55	6.31
Wrinkled	6.29	88.1

The measured area was 20 μm × 20 μm

R_a average surface roughness, P_v peak value of surface roughness

process. Another possible reason is the effect of the thermal deposition process of the thin platinum layer required for SEM observation. Therefore, as shown in Fig. 5c, the surface roughness of the replicated PDMS surface was measured using large-area atomic force microscopy (AFM) (SII Nano Technology) and compared with the native PDMS surface as a comparable surface. Table 1 summarizes the measured data; briefly, the average and peak values of the surface roughness of the PDMS surface increased with the thermal curing process of liquid PDMS on cured PDMS.

2.4 Static valve operation

Figure 6 shows the fabricated typical valve with a fluid chamber having a rectangular cross section (a) and the proposed pneumatic valve with a spherical dome-shape chamber (b). Blue ink was introduced into the valve structures to visualize the valve operation before (1) and after (2)

pneumatic actuation. The height of the channel and chamber of the typical valve were 55 μm. The thickness of the fabricated valve diaphragm was 100 μm. A pressure step of 100 kPa was applied to the valves using compressed air. The optical images clearly showed that there were some leakage paths in the typical valve. However, the proposed valve closed off the fluid path; no continuous fluidic path remained. In short, the proposed valve structure with a spherical dome-shape liquid chamber was more effective than the typical valve with a rectangular chamber, as expected.

3 Results and discussion

3.1 Flow rate

Figure 7 shows the measured temporal response of the liquid flow rectified by the valves. A laboratory-designed pneumatic system (Lee et al. 2013) was used to control valve operation and supply a continuous fluid flow from a glass bottle into the fabricated valve chip. A digital microscope and a liquid flow sensor (Sensirion, ASL1600 liquid mass flow meter) were used to observe valve operation and measure the fluid flow. The sampling time was 80 ms, and the best resolution was 0.025 μL/min at 12.5 Hz. The accuracy was 3 % of the measured value.
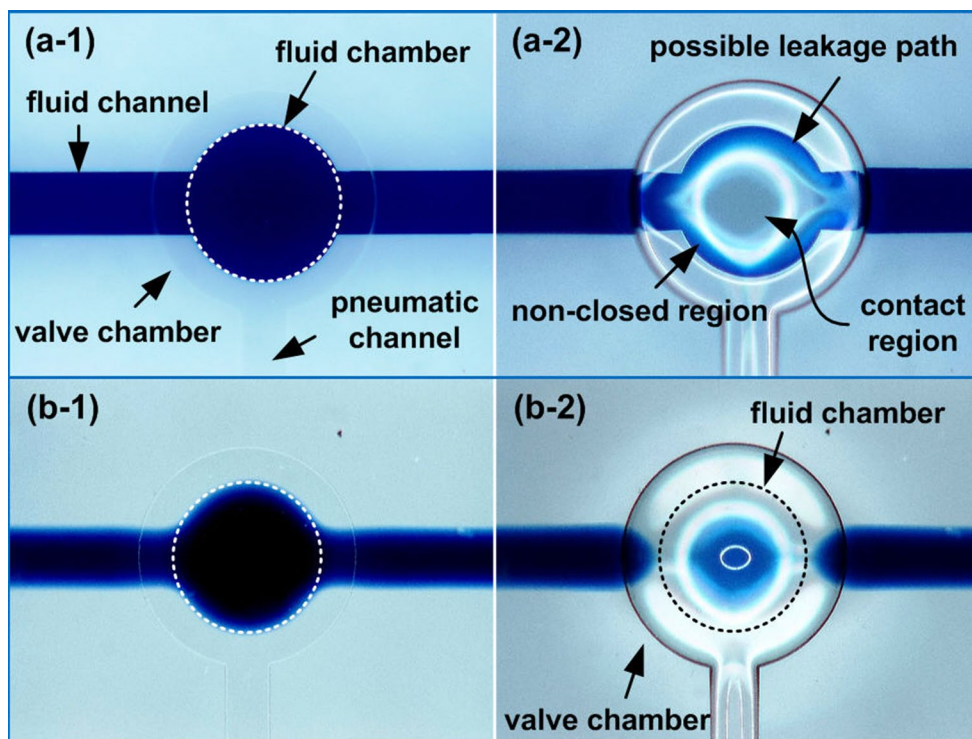

Fig. 6 Fabricated **a** proposed and **b** typical valves. *1* and *2* correspond to before and after actuation, respectively
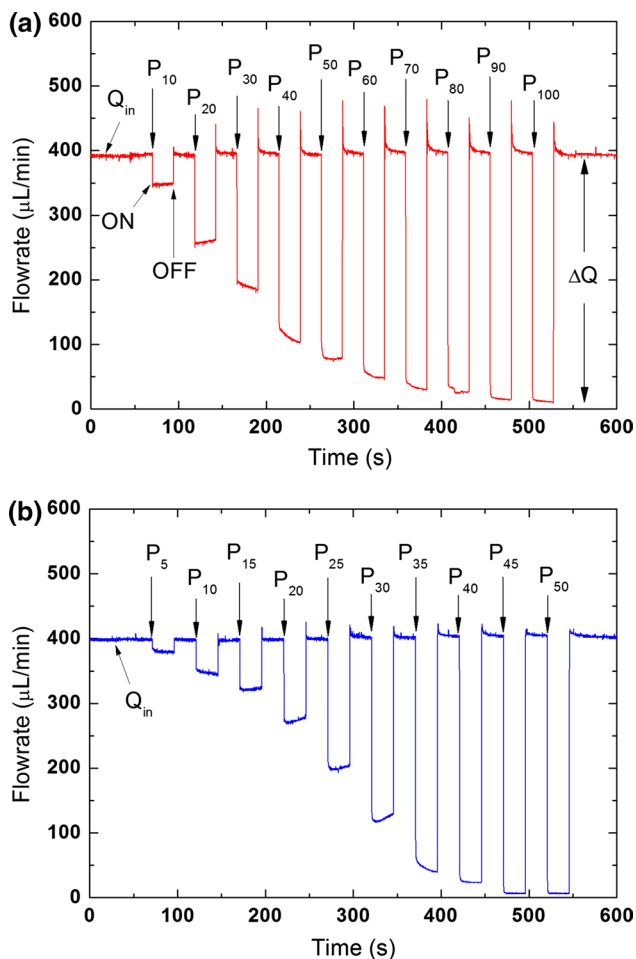
Fig. 7 Temporal responses of flow rates rectified by the **a** typical and **b** proposed valves. P_x represents applied pressure of x kPa for valve operation. The pressure was increased in increments of 10–100 kPa in **a** and 5–50 kPa for **b**. Q_{in} introduced flow rate; ΔQ rectified flow rate during valve operation

Pressure-driven water was introduced into the valve at a constant flow rate of 400 μL/min, and the flow variations were measured with the flow sensor while a programmed square-wave pressure for on/off control of the valve was applied to the valve chamber. Figure 7a shows that the magnitude of the applied first pressure, P_{10}, for the typical valve was 10 kPa and increased in increments of 10–100 kPa. In the case of the proposed valve shown in Fig. 7b, a pressure of 5 kPa (P_{05}) was first applied and then increased in increments of 5–50 kPa. The flow rate was reduced by the deformed valve diaphragms during operation of the pneumatic valves.

One finding was that the measured flow rates rectified by the typical valve decreased gradually and then saturated as the applied pressure was increased to 100 kPa. However, for the proposed valve, the flow rates decreased markedly when the applied pressure was increased to 50 kPa. They

were close to zero at applied pressures of P_{45} and P_{50}. The experimental results indicated that the proposed valve effectively blocked the fluidic path of the working fluid under relatively low operational pressures.

3.2 Valve efficiency

Figure 8 shows the valve efficiency of the typical and proposed valves as a function of the applied operational pressures. The valve efficiency was defined as the ratio of the flow rate difference (ΔQ) to the introduced flow rate (Q) and was calculated from the measured temporal responses, as shown in Fig. 7. Pressure-driven liquid flows with various flow rates ranging from 200 to 500 μL/min were introduced into the valve chips.

When the introduced flow rate was 200 μL/min, the efficiency of the proposed valve was larger than that of the typical valve. For example, at an applied pressure of 40 kPa, the valve efficiencies of the typical and proposed valves were 65 and 97 %, respectively. The efficiency of the proposed valve increased rapidly and then saturated as the applied pressure was increased. However, the efficiency of the typical valve gradually increased and then saturated; unlike the proposed valve, it was difficult to achieve an efficiency of 100 % under the applied pressure range. As the introduced flow rate increased, the efficiency of the proposed valve became less than that of the typical valve at lower pressures; however, at higher pressures, the efficiency of the proposed valve was much greater.

4 Discussion

The results presented above were caused by the structural constraints of the valve chamber. During operation of the typical valve, the flexible PDMS diaphragm deformed and then contacted to the shallow fluid chamber. Thus, a large amount of the flow rate was blocked by the valve operation at lower pressures. However, the flow rate rectified by the typical valve was saturated under high pressures because the deformation of the valve diaphragm was restricted by the rectangular shape of the fluid chamber. Therefore, even when higher pressure was applied to operate the typical valve, possible leakage paths of the pressure-driven flow around the rectangular shape of fluid chamber still existed, as shown in Fig. 6a2. It was difficult to block the liquid flow effectively. For the proposed valve, the diaphragm could not close the fluid path in the spherical dome-shape fluid chamber at low pressures. However, the proposed valve could block the pressure-driven fluid as the valve diaphragm closed off the fluid flow in the spherical dome-shape fluid chamber when it was fully inflated, as shown in Fig. 6b2.

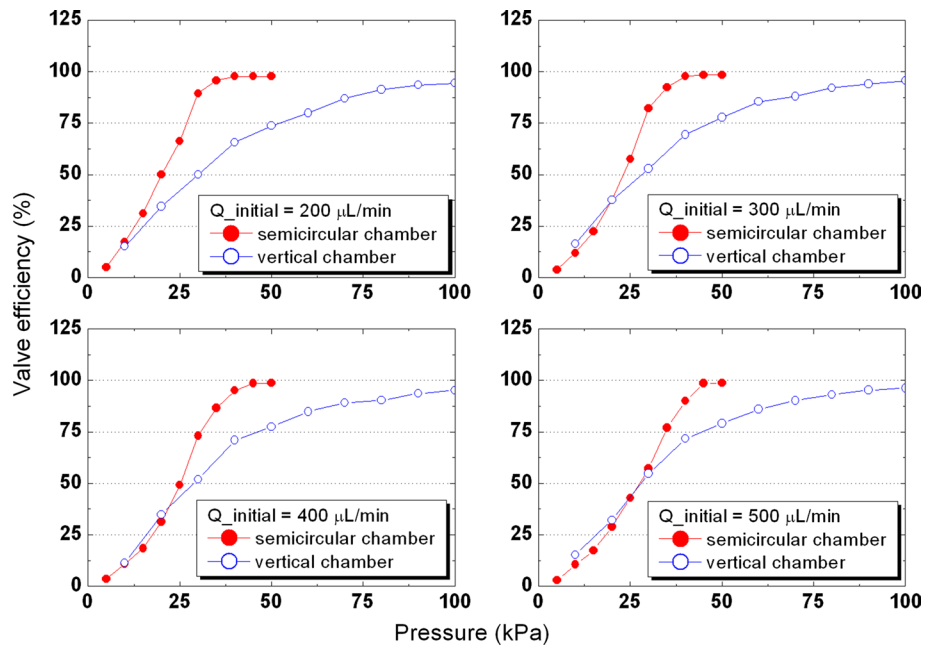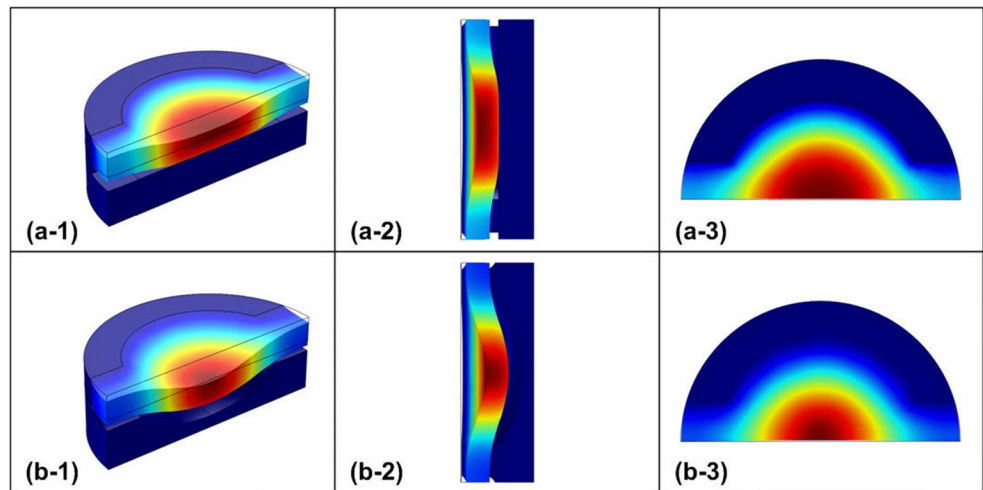**Fig. 8** Valve efficiency as a function of applied pressure

Fig. 9 Structural analysis results of the typical (**a**) and the proposed (**b**) valve diaphragm. (*1*) Three-dimensional view of the vertical displacement of the deformed valve diaphragm, (*2*) *z*–*x* plane view, and (*3*) *x*–*y* plane view

4.1 FEM analysis

Three-dimensional structural analysis of the valves was performed using the finite element method (FEM) tool FEMLAB (Comsol Inc.) to examine the flow characteristics. A deformable PDMS valve diaphragm was simulated using a linear elastic material model with a linear relationship between stress and strain. Considering the height of the fluid chamber, the valve diaphragm was deformed in the small strain region of the PDMS (Kim et al. 2011). Thus, we could use a linear elastic material model for the PDMS in our structural analysis of the valve diaphragm. Young's modulus and Poisson's ratio for the PDMS were set to 664.5 kPa and 0.45, respectively (Kim et al. 2011).

The dimensions of the FEM model for each device were the same as those of the fabricated devices shown in Fig. 5.

Figure 9 shows a three-dimensional view of the vertical displacement of the deformed valve diaphragm when a pressure of 40 kPa was applied to the valves. The deformation of the typical valve was restricted by the flat fluid chamber layer, while the proposed valve with a spherical dome-shape fluid chamber was fully deformed. As the valve chamber was larger than the fluid chamber, the valve diaphragm covering some part of the channel region was also deformed. This could be an effective structural design for blocking fluid by increasing the fluidic resistance in the micro-channel due to deformation of the diaphragm (Jeong and Konishi 2008).

Figure 10 shows the vertical displacement of the valve diaphragm under various applied pressures. The displacement of the typical valve was limited by the depth of the fluid channel and chamber region. Thus, the typical valve diaphragm was deformed and then made contact with the center of the fluid chamber when a pressure of 20 kPa was applied. As the pressure was increased, the contact region expanded, but it was difficult to close off the fluid chamber region completely, even when excessive pressure was applied. But, the efficiency of the typical valve should approach that of the proposed one while the height of the fluid channel and the thickness of the valve diaphragm were decreased. These dimensions of the channel and chamber structure for the typical valve are comparable to those of the pneumatic valves (Kim et al. 2011). For the proposed valve with a spherical dome-shape fluid chamber, the valve diaphragm was fully inflated. As the height of the

fluid channel was less than that of the spherical dome-shape fluidic chamber, the deformed diaphragm first covered the interfacial region of the fluid channel and the upper part of the fluid chamber. The fluidic resistance in the channel and the chamber was increased because the fluidic path of the working fluid narrowed as the pressure increased. Thus, the working fluid was blocked by the structural deformation of the valve diaphragm.

5 Conclusions

This paper describes a fabrication method for a pneumatic valve with a curved fluidic structure. During the thermal curing process of the liquid PDMS for the spherical dome-shape fluidic PDMS structure, the flexible diaphragm of the prepared PDMS mold was inflated by the increasing pressure in the sealed cavity, and the physical shape of the deformed diaphragm was transferred to the liquid PDMS. Thus, a spherical dome-shape fluid chamber could be fabricated using a typical curing process with a hot plate.

The proposed pneumatic valve with a curved chamber was fabricated after bonding the valve chamber to the diaphragm. Its operation was observed with a microscope using colored ink as the working fluid to highlight the valve shapes. We confirmed that the proposed valve was more effective than a valve with a typical rectangular cross section. Measurements of the temporal response of liquid flow rectified by the proposed pneumatic valve demonstrated that the proposed valve could fully close off the fluid flow at lower operational pressures than a typical vale with a fluid chamber having a rectangular cross section. The effectiveness of the proposed valve structure was also verified through FEM analysis.

The proposed fabrication method provides a simple and useful means to overcome the drawbacks of fluid microchannels with rectangular cross sections, allowing us to fabricate micro-fluidic devices with spherical dome-shape fluid structures, such as a channel, valve, actuator, or membrane micro-pump.

Fig. 10 Vertical displacement of the valve diaphragm under various applied pressures: **a** typical valve and **b** proposed valve (*1* height of the fluid channel and chamber, *2* channel region, *3* chamber region, *4* height of the spherical channel)

References

Bae B, Kim N, Kee H, Kim SH, Lee Y, Lee S, Park K (2002) Feasibility test of an electromagnetically driven valve actuator for glaucoma treatment. J Microelectromech Syst 11:344

Cherng Y, Su GJ (2014) Fabrication of polydimethylsiloxane microlens array on spherical surface using multi-replication process. J Micromech Microeng 24:015016
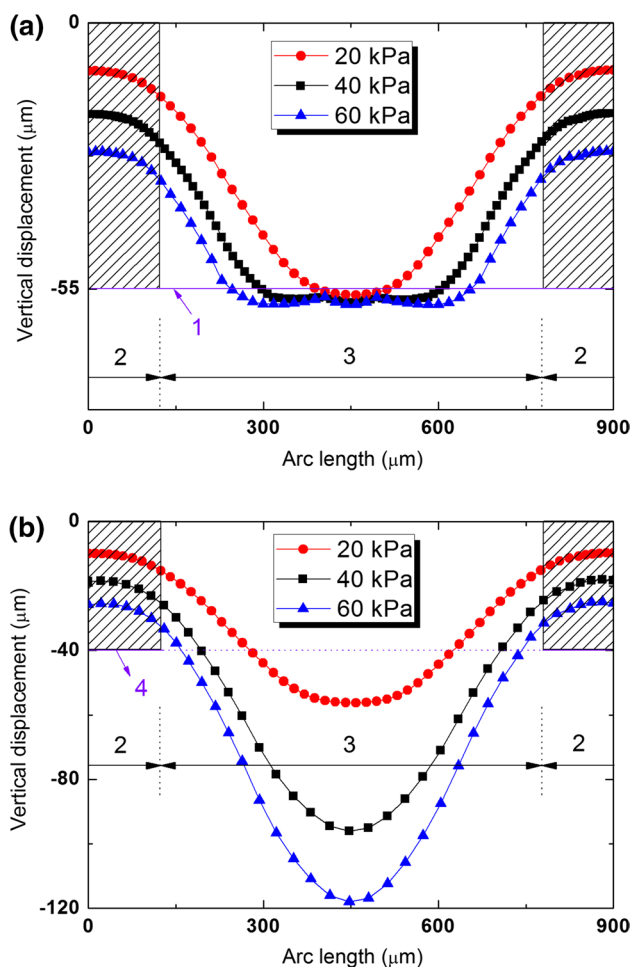
Dy A, Cosmanescu A, Sluka J, Glazier JA, Stupack D, Amarie D (2014) Fabricating microfluidic valve master molds in SU-8 photoresist. J Micromech Microeng 24:057001

Fordyce PM, Diaz-Botia CA, DeRisia JL, Gomez-Sjoberg R (2012) Systematic characterization of feature dimensions and closing pressures for microfluidic valves produced via photoresist reflow. Lab Chip 12:4287

Fu AY, Chou HP, Spence C, Arnold FH, Quake SR (2002) An integrated microfabricated cell sorter. Anal Chem 74:2451

Goettsche T, Kohnle J, Willmann M, Ernst H, Spieth S, Tischler R, Messner S, Zengerle R, Sandmaier H (2005) Novel approaches to particle tolerant valves for use in drug delivery systems. Sens Actuators, A 118:70

Goll C, Bacher W, Bustgens B, Maas D, Ruprecht R, Schomburg WK (1997) An electrostatically actuated polymer microvalve equipped with a movable membrane electrode. J Micromech Microeng 7:224

Grover WH, Skelley AM, Liu CN, Lagally ET, Mathies RA (2003) Monolithic membrane valves and diaphragm pumps for practical large-scale integration into glass microfluidic devices. Sens Actuators, B 89:315

Ho CM, Yang X, Grosjean C, Tai YC (1998) A MEMS thermopneumatic silicone rubber membrane valve. Sens Actuators, A 64:8

Hosokawa K, Maeda R (2000) A pneumatically-actuated three-way microvalve fabricated with polydimethylsiloxane using the membrane transfer technique. J Micromech Microeng 10:415

Huang S, He Q, Hu X, Chen H (2012) Fabrication of micro pneumatic valves with double-layer elastic poly (dimethylsiloxane) membranes in rigid poly (methyl methacrylate) microfluidic chips. J Micromech Microeng 22:085008

Jeong OC, Konishi S (2008) Fabrication of a peristaltic micro pump with novel cascaded actuators. J Micromech Microeng 18:025022

Jeong KH, Liu GL, Chronis N, Lee LP (2004) Tunable microdoublet lens array. Opt Express 12(11):2494

Kim HT, Kim JK, Jeong OC (2011a) Hydrophilicity of surfactant-added poly (dimethylsiloxane) and its applications. Jpn J Appl Phys 50:06GL04

Kim TK, Kim JK, Jeong OC (2011b) Measurement of nonlinear mechanical properties of PDMS elastomer. Microelectron Eng 88:1982

Kim TK, Lee SW, Ahn JY, Laurell T, Kim S, Jeong OC (2011c) Fabrication of Microfluidic platform with optimized fluidic network toward on-chip parallel systematic evolution of ligands by exponential enrichment process. Jpn J Appl Phys 50:06GL05

Lee SW, Kang J, Ren S, Laurell T, Kim S, Jeong OC (2013) A cross-contamination-free SELEX platform for a multi-target selection strategy. BioChip J 7(1):38

Li HQ, Roberts DC, Steyn JL, Turner KT, Yaglioglu O, Hagood NW, Spearing SM, Schmidt MA (2004) Fabrication of a high frequency piezoelectric microvalve. Sens Actuators, A 111:51

Liu J, Enzelberger M, Quake S (2002) A robust and scalable microfluidic metering method that allows protein crystal growth by free interface diffusion. Electrophoresis 23:1531

McDonald JC, Whitesides GM (2002) Poly (dimethylsiloxane) as a material for fabricating microfluidic devices. Acc Chem Res 35:491

Oh KW, Rong R, Ahn CH (2005) Miniaturization of pinch-type valves and pumps for practical micro total analysis system integration. J Micromech Microeng 15:2449

Park W, Han S, Kwon S (2010) Fabrication of membrane-type microvalves in rectangular microfluidic channels via seal photopolymerization. Lab Chip 10:2814

Rich CA, Wise KD (2003) A high-flow thermopneumatic microvalve with improved efficiency and integrated state sensing. J Microelectromech Syst 12:8

Sato K, Shikida M (1994) An electrostatically actuated gas valve with an S-shaped film element. J Micromech Microeng 4:205

Studer V, Hang G, Pandolfi A, Ortiz M, Anderson WF, Quake SR (2004a) Scaling properties of a low-actuation pressure microfluidic valve. J Appl Phys 95:393

Studer V, Jameson R, Pellereau E, Pepin A, Chen Y (2004b) A microfluidic mammalian cell sorter based on fluorescence detection. Microelectron Eng 73:852

Sundararajan N, Kim D, Berlin AA (2005) Microfluidic operations using deformable polymer membranes fabricated by single layer soft lithography. Lab Chip 5:350

Takao H, Miyamura K, Ebi H, Ashiki M, Sawada K, Ishida K (2005) A MEMS microvalve with PDMS diaphragm and two-chamber configuration of thermo-pneumatic actuator for integrated blood test system on silicon. Sens Actuators, A 119:75

Thorsen T, Maerkl SR, Quake SR (2002) Microfluidic large-scale integration. Science 298:580

Unger MA, Chou HP, Thorsen T, Scherer A, Quake SR (2000) Monolithic microfabricated valves and pumps by multilayer soft lithography. Science 288:113

Wang YC, Choi MN, Han JY (2004) Two-dimensional protein separation with advanced sample and buffer isolation using microfluidic valves. Anal Chem 76:4426

Whitesides GM (2006) The origins and the future of microfluidics. Nature 442:368

Yanagisawa K, Kuwano H, Tapo A (1993) An electromagnetically driven microvalve. Proc Transducers 93:102

Yang X, Holke A, Jacobson SA, Lang JH, Schmidt MA, Umans SD (2004a) An electrostatic, on/off microvalve designed for gas fuel delivery for the MIT microengine. J Microelectromech Syst 13:660

Yang EH, Lee C, Mueller J, George T (2004b) Leak-tight piezoelectric microvalve for high-pressure gas micropropulsion. J Microelectromech Syst 13:799